An interferometric interpretation of Marchenko redatuming including free-surface multiples

Staring, Myrna; van der Neut, Joost; Wapenaar, Kees

DOI
10.1190/segam2016-13956290.1

Publication date
2016

Document Version
Accepted author manuscript

Published in
SEG Technical Program Expanded Abstracts 2016

Citation (APA)
Staring, M., van der Neut, J., & Wapenaar, K. (2016). An interferometric interpretation of Marchenko redatuming including free-surface multiples. In C. Sicking, & J. Ferguson (Eds.), *SEG Technical Program Expanded Abstracts 2016* (pp. 5172-5176). (SEG Technical Program Expanded Abstracts; Vol. 2016). SEG. https://doi.org/10.1190/segam2016-13956290.1

An interferometric interpretation of Marchenko redatuming including free-surface multiples

Myrna Staring, Joost van der Neut and Kees Wapenaar (Delft University of Technology)

SUMMARY

We present an interferometric interpretation of the iterative Marchenko scheme including both free-surface multiples and internal multiples. Cross-correlations are used to illustrate the combination of causal and acausal events that are essential for the process of multiple removal. The first 4 steps in the scheme are discussed in detail, where the effect of different contributions on the result is displayed and the formation of individual events is illustrated. We highlight the events that are necessary to understand the process that removes both internal multiples and free-surface multiples from the data. We demonstrate that additional contributions are needed to correct for the presence of free-surface multiples.

INTRODUCTION

The Marchenko methodology was proven to be successful for the elimination of internal multiples from seismic data (Broggini et al., 2012; Wapenaar et al., 2014). Recently, this methodology was adjusted to also incorporate free-surface multiples (Singh et al., 2015). To initiate the scheme, one needs the reflection response $\overline{R}$ at the surface, recorded due to a source at the surface, in combination with a depth-level indication specified in one-way traveltime. Representations that relate the one-way Green's functions to the one-way focusing functions were adjusted to include the reflection coefficient r at the free-surface (Singh et al., 2015):

$$\begin{aligned}\overline{G}^-(\mathbf{x_i}',\mathbf{x_0}'',\omega) = \int_{\partial D_0} \Big[& f_1^+(\mathbf{x_0},\mathbf{x_i}',\omega)\overline{R}(\mathbf{x_0},\mathbf{x_0}'',\omega) \\ & - r f_1^-(\mathbf{x_0},\mathbf{x_i}',\omega)\overline{R}(\mathbf{x_0},\mathbf{x_0}'',\omega)] dx \\ & - f_1^-(\mathbf{x_0}'',\mathbf{x_i}',\omega),\end{aligned} \tag{1}$$

$$\begin{aligned}\overline{G}^+(\mathbf{x_i}',\mathbf{x_0}'',\omega) = - \int_{\partial D_0} \Big[& f_1^-(\mathbf{x_0},\mathbf{x_i}',\omega)^*\overline{R}(\mathbf{x_0},\mathbf{x_0}'',\omega) \\ & - r f_1^+(\mathbf{x_0},\mathbf{x_i}',\omega)^*\overline{R}(\mathbf{x_0},\mathbf{x_0}'',\omega)] dx \\ & + f_1^+(\mathbf{x_0}'',\mathbf{x_i}',\omega)^*,\end{aligned} \tag{2}$$

where ∂D_0 is the surface interface above which the medium is homogeneous, $\overline{G}^-$ and $\overline{G}^+$ represent the upgoing and downgoing Green's functions that include multiples, and f_1^- and f_1^+ signify the upgoing and downgoing focusing functions. The bar above a character indicates the presence of free-surface multiples. Furthermore, $\mathbf{x_0}$, $\mathbf{x_0}''$ and $\mathbf{x_i}'$ represent spatial positions on the surface interface, just above the surface interface and at the redatuming level respectively. The $*$ denotes complex conjugation. The reflection coefficient of the free surface r is assumed to be equal to -1. The expressions for $\overline{G}^-$ and $\overline{G}^+$ can be used to create an image without artifacts from internal multiples and free-surface multiples. We discretize equations 1 and 2 and write them in matrix form, similar to van der Neut et al. (2015a):

$$\begin{pmatrix} -\overline{g}^- \\ \overline{g}^{+*} \end{pmatrix} = \begin{pmatrix} I + r\overline{R} & -\overline{R} \\ -\overline{R}^* & I + r\overline{R}^* \end{pmatrix} \left(\begin{pmatrix} 0 \\ f_{1d}^+ \end{pmatrix} + \begin{pmatrix} f_1^- \\ f_{1m}^+ \end{pmatrix} \right). \tag{3}$$

The downgoing focusing function has been split in a direct term f_{1d}^+ and a coda f_{1m}^+. These matrices contain 2 equations and 4 unknowns, namely $-\overline{g}^-$, $\overline{g}^{+*}$, f_1^- and f_{1m}^+ (Wapenaar et al., 2014; van der Neut et al., 2015b). According to the standard Marchenko methodology, the window function Θ can be applied to reduce the number of unknowns to the two focusing functions only. This time-symmetric windowing function utilizes the difference in causality properties to separate the Green's function from the focusing function. After applying the filter and rearranging the terms, the following expression is obtained:

$$\begin{pmatrix} -r\Theta\overline{R} & \Theta\overline{R} \\ \Theta\overline{R}^* & -r\Theta\overline{R}^* \end{pmatrix} \begin{pmatrix} 0 \\ f_{1d}^+ \end{pmatrix} = \begin{pmatrix} I + r\Theta\overline{R} & -\Theta\overline{R} \\ -\Theta\overline{R}^* & I + r\Theta\overline{R}^* \end{pmatrix} \begin{pmatrix} f_1^- \\ f_{1m}^+ \end{pmatrix}. \tag{4}$$

We can recognize this as a Fredholm integral equation of the second kind, which we rewrite as a Neumann series:

$$\begin{pmatrix} f_1^- \\ f_{1m}^+ \end{pmatrix} = \sum_{k=1}^{\infty} \begin{pmatrix} -r\Theta\overline{R} & \Theta\overline{R} \\ \Theta\overline{R}^* & -r\Theta\overline{R}^* \end{pmatrix}^k \begin{pmatrix} 0 \\ f_{1d}^+ \end{pmatrix}. \tag{5}$$

This equation is applied to iteratively solve the coupled Marchenko equations including free-surface multiples. This scheme is exactly the same as the iterative scheme proposed by Singh et al. (2015). Following van der Neut et al. (2015b), we now intuitively interpret the iterative process in terms of correlations and convolutions. One iteration will update both the upgoing and downgoing focusing functions (see equation 5). In order to provide a clear interpretation, one iteration is split into two separate steps, in which either the upgoing or downgoing functions are updated.

APPLICATION

We use a simple 1D model, in order to provide an interpretation that is as uncomplicated and intuitive as possible. It contains a free-surface and three interfaces at depths of 1000 m, 1750 m and 2675 m. The model has a constant velocity of 2500 m/s. The density varies per layer, with densities of 1000 kg/m^3 for the first and third layer, 2000 kg/m^3 for the second layer and 1100 kg/m^3 for the fourth layer. Figure 1a displays the 1D model, including one-way traveltimes between the interfaces. We place the redatuming level at 2250 m, indicated by the dotted line. Figure 1b shows the reflection response, obtained by simulation with a reflectivity code, where both source and receiver were placed at the surface. The generated synthetics show primary arrivals at A and B, free-surface multiples at $\overline{C}$, $\overline{E}$ and $\overline{F}$, and an internal multiple at D.

Step 1: $f_1^- = \Theta\overline{R}f_{1d}^+$

The first step involves a cross-correlation of the reflection response with the direct wave. Intuitively, one can view this as

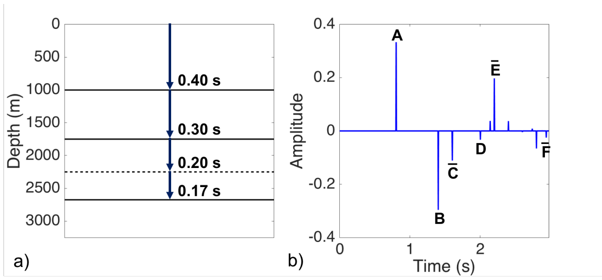

Figure 1: (a) Image of the layered 1D model with 3 interfaces. (b) Reflection response recorded at the surface.

a backward shift of the reflection response in time. The size of the shift is dictated by the one-way traveltime to the redatuming level. Next, the windowing function Θ is applied, separating the upgoing focusing function from the upgoing Green's function. The result is shown in Figure 2, displaying the focusing function on the left and the Green's function on the right, separated by the black vertical line. Only selected events are shown for simplicity. The focusing function contains events M, N and $\overline{O}$. Figure 3 explains the formation of these virtual (non-physical) events, that contain both causal and acausal paths. Causal travelpaths are indicated in red, acausal paths are colored green. The time-reversed direct wave f^+_{1d} is labeled as H^*. Events M and N are the result of primary reflections A and B correlated with the direct wave, similar to events found in the original scheme (see van der Neut et al. 2015b). These desired events will play an essential role in step 3, where they will be used for the removal of undesired events in the upgoing Green's function. Event $\overline{O}$ was created by the correlation of free-surface multiple $\overline{C}$ with the direct wave. Since the final focusing function should not include any free-surface multiples or their derivatives, the iterative scheme aims to cancel this event in next iterations. As the event has not yet been canceled in this step, it will produce undesired events in the next step.

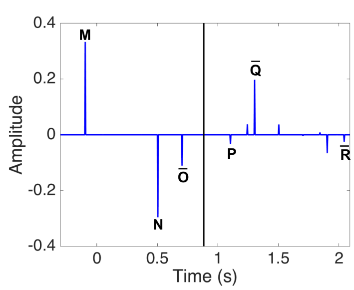

Figure 2: Image showing the result of step 1. The windowing function Θ is indicated by the black vertical line. Left of the window: the upgoing focusing function. Right of the window: the upgoing Green's function.

Figure 4 illustrates the events in the upgoing Green's function, at the right side of the windowing filter. Arrival P is a virtual event created by internal multiple D, comparable to an event found in the original scheme. Event $\overline{Q}$ is a virtual event generated by free-surface multiple $\overline{E}$. When a Green's function containing these events were to be used for imaging, a reflector would be incorrectly placed at depth levels corresponding to these traveltimes. Therefore, events P and $\overline{Q}$ are undesired and should be canceled by the scheme. Correct upgoing events in this Green's function can also be observed, for example event $\overline{R}$. After the first step, the Green's function should already contain all its physical upgoing primary reflections and multiple reflections with correct amplitudes. However, there are still non-physical events that pollute the Green's function caused by both internal multiples and free-surface multiples. Future iterations will only cancel these undesired events, while leaving the desired events intact.

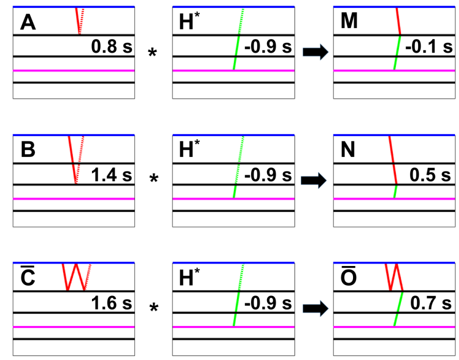

Figure 3: Illustrations of the events in the upgoing focusing function after step 1.

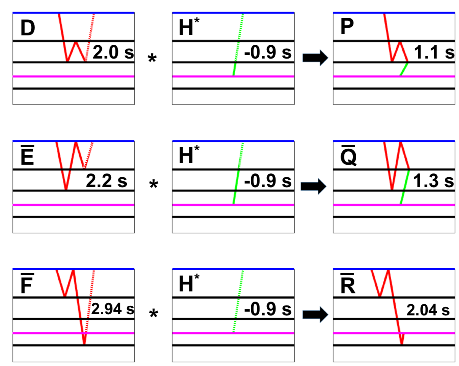

Figure 4: Illustrations of the events in the upgoing Green's function after step 1.

Step 2: $f^+_{1m} = \Theta\overline{R}^* f^-_1 + \Theta\overline{R}^* f^+_{1d}$

This step gives a first estimate of the coda of the downgoing focusing function, by summing a cross-correlation and a convolution. Figure 5 displays the resulting coda of the downgoing focusing function and the time and polarity reversed Green's function including the direct wave (see equation 3). The contributions of the first term are displayed in blue, while the contributions of the second term are displayed in red. Note that the second term ($\Theta\overline{R}^* f^+_{1d}$) does not contribute to the focusing function, it only contributes to the Green's function. The illustrations in figure 6 explain the origin of events $\overline{U}$, V and $\overline{W}$

in the focusing function. Undesired event $\overline{O}$ from the upgoing focusing function of step 1 has created two undesired events in the coda of the downgoing focusing function (events $\overline{U}$ and $\overline{W}$). Event V is correct, resulting from the cross-correlation of primary reflections B and A with the direct wave. This event is essential for the removal of undesired events in both the upgoing and downgoing Green's functions in steps 3 and 4.

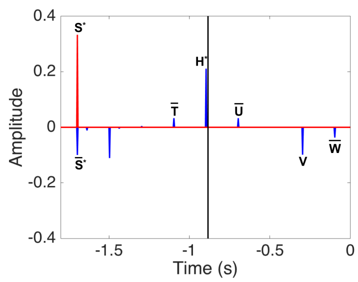

Figure 5: Image showing the result of step 2. Left: the downgoing Green's function and the time-reversed direct wave. Right: the downgoing focusing function.

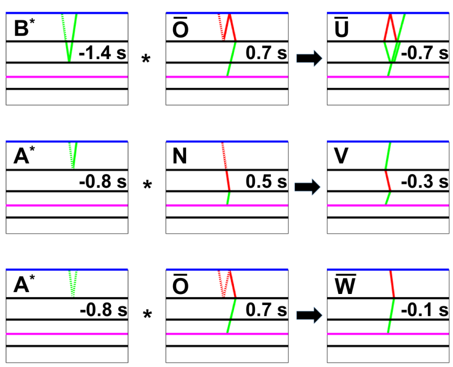

Figure 6: Illustrations of the events in the downgoing focusing function after step 2.

On the left of the filter are the downgoing Green's function and the time-reversed direct wave H^*. Figure 7 explains the events in the Green's function due to the first term ($\Theta R^* f_1^-$) and the second term ($\Theta R^* f_{1d}^+$). Events $\overline{S}^*$ and $\overline{T}$ originate from the first term, while event S^* results from the second term. Event $\overline{T}$ exists from the cross-correlation of free-surface multiple $\overline{C}$ with primary arrival B and the direct wave. It is a virtual event that should be canceled in future iterations. Events $\overline{S}^*$ and S^* arrive at the same time, but have opposite polarity. Note that event $\overline{S}^*$ was created by correlating free-surface multiple $\overline{C}$ with primary arrival A and the direct wave, while event S^* exists due to correlation of time-reversed primary event A^* with the direct wave. This is where the scheme of Singh et al. (2015) differs from the original Marchenko scheme without free-surface multiples. A second term is present that directly modifies the amplitudes of events in the downgoing Green's function to obtain a correct amplitude. A third term will be added in the next iteration. At the end of the second step, all downgoing multiples are present in the Green's function. Future steps will remove undesired events and update the amplitudes of desired events.

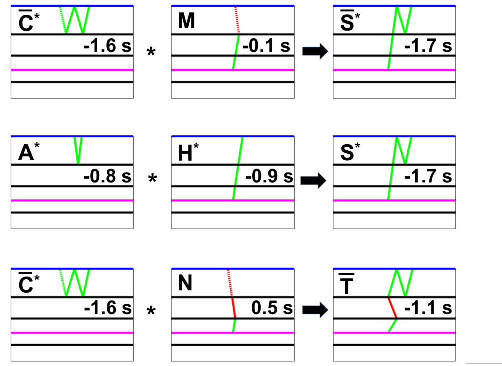

Figure 7: llustrations of the events in the downgoing Green's function after step 2. Events $\overline{S}^*$ and $\overline{T}$ originate from the first term, while event S^* results from the second term.

Step 3: $f_1^- = \Theta \overline{R} f_{1d}^+ + \Theta \overline{R} f_{1m}^+ + \Theta \overline{R} f_1^-$

In the third step, three terms update the upgoing focusing function. Figure 8 displays the resulting upgoing focusing function and upgoing Green's function. Contributions from the first term $\Theta \overline{R} f_{1d}^+$ are displayed in blue, events from the second term $\Theta \overline{R} f_{1m}^+$ are red and contributions from the third term $\Theta \overline{R} f_1^-$ can be observed in green. The events in the first term were discussed in step 1, see Figures 3 and 4 for reference. When studying the second term, one can observe that a small virtual event $\overline{X}$ has been added to the upgoing focusing function in figure 8, due to virtual event $\overline{U}$ in the coda of the downgoing focusing function f_{1m}^+, which was in turn created by undesired event $\overline{O}$ in the upgoing focusing function. An event similar to event $\overline{X}$ cannot be found in the original scheme without free-surface multiples, it is purely an artifact of the new scheme that will be removed in future iterations. Event Y in the Green's function has the exact same origin.

Event $\overline{O}$ was first found in step 1 (see figure 3). Figure 9 shows that the second and third terms now also start contributing to this event. The first and second term create event $\overline{O}$ from a recipe including a free-surface multiple. The third term generates event O with opposite polarity. It was created by the convolution of primary event A with desired event M in the upgoing focusing function from step 1. This can be interpreted as a form of multiple prediction. When adding the three terms, events $\overline{O}$ and O should cancel out. The exact same method is applied to remove event $\overline{Q}$ from the upgoing Green's function. In addition, a similar method is applied for the removal of event P, created by correlation of internal multiple D with the direct wave in step 1. Figure 9 illustrates the formation of another event P with opposite polarity. Now an event from the downgoing focusing function is used to remove an undesired event in the upgoing Green's function. Again, this can be seen as a form of multiple prediction.

Note that both the upgoing focusing function and the upgoing Green's function already contained all correct arrivals from step 1 onwards. From the observations in this step, it can be concluded that the second term appears to be essential for the removal of undesired events due to internal multiples in the first term, while the third term corrects for undesired events created by free-surface multiples in both the first and the second term. Undesired events in the upgoing focusing function and Green's function are removed using desired events from both the upgoing and the downgoing focusing functions obtained in previous steps.

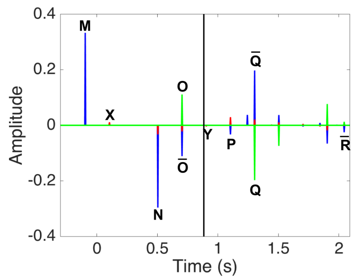

Figure 8: Image showing the result of step 3. Left: the upgoing focusing function. Right: the upgoing Green's function.

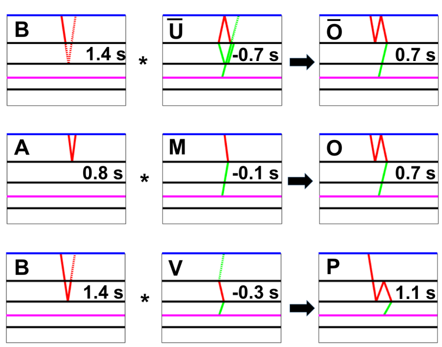

Figure 9: llustrations of the events in the upgoing focusing function and Green's function after step 3. Events $\overline{O}$ and P are found in the second term, while event O is a contribution of the third term.

Step 4: $f^+_{1m} = \Theta R^* f^-_1 + \Theta R^* f^+_{1d} + \Theta R^* f^+_{1m}$

Step 4 now adds a third term to update the downgoing focusing function. Figure 10 displays the downgoing focusing function and Green's function that contain all three terms. The focusing function contains the exact same events as in step 2 (see figure 6), but note that the amplitudes of undesired events $\overline{U}$ and $\overline{W}$ have decreased. This is the result of the cancellation of event $\overline{O}$ in the previous step. Therefore, undesired events in the downgoing focusing function were implicitly suppressed by cancellation in the upgoing focusing function of the previous step. Future iterations will completely remove these undesired events.

In the Green's function, event S^* has gained an extra contribution from the newly introduced third term (the green event in figure 10). All three terms now cooperate to obtain the correct amplitude of this desired event. Figure 11 illustrates the creation of event T, which has opposite polarity to the event $\overline{T}$ in step 2 (see figure 7). Event $\overline{T}$ exists due to the correlation of time-reversed free-surface multiple $\overline{C}$ with primary B and the direct wave, while event T was formed by the correlation of two primaries and the direct wave. When these two terms are added, undesired event $\overline{T}$ is canceled by event T. Note that event T was created by event V, a desired event in the downgoing focusing function. Thus, the downgoing focusing function from the previous update was used to remove an undesired event from the Green's function. This is comparable to the removal of event $\overline{O}$ with the upgoing focusing function in step 3.

When continuing iterations after step 4, undesired events will be completely removed from the focusing functions. In addition, Green's functions without virtual events are obtained. Desired events in the downgoing Green's function will be adjusted to the correct amplitude.

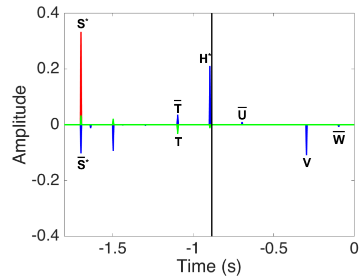

Figure 10: Image showing the result of step 4. Left: the downgoing Green's function. Right: the downgoing focusing function.

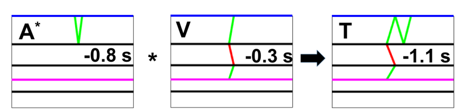

Figure 11: llustrations of event T in the downgoing Green's function. It originates from the third term.

CONCLUSION

The Marchenko scheme including free-surface multiples alternates between updating the upgoing fields and downgoing fields, similar to the original scheme. However, extra terms due to the reflection coefficient r at the free-surface complicate the process. Both the upgoing and downgoing focusing functions are now employed to remove undesired events in the one-way Green's functions, created by free-surface multiples and internal multiples. The upgoing Green's function contains all correct physical events from the start. This enables adaptive subtraction for the removal of non-physical events added by multiples. Contributions from both the upgoing and the downgoing focusing functions cooperate to create physical events with correct amplitudes in the downgoing Green's function. In addition, the iterative scheme initially contaminates both the upgoing focusing function and Green's function with undesired non-physical events that are canceled in later iterations.

ACKNOWLEDGMENTS

This research has been performed in the framework of the project ”Marchenko imaging and monitoring of geophysical reflection data”, financially supported by the Dutch Technology Foundation STW, applied science division of NWO and the Technology Program of the Ministry of Economic Affairs.

REFERENCES

Broggini, F., R. Snieder, and K. Wapenaar, 2012, Focusing the wavefield inside an unknown 1d medium: Beyond seismic interferometry: Geophysics, **77**, A25–A28.

Singh, S., R. Snieder, J. Behura, J. van der Neut, K. Wapenaar, and E. Slob, 2015, Marchenko imaging: Imaging with primaries, internal multiples, and free-surface multiples: Geophysics, **80**, S165–S174.

van der Neut, J., J. Thorbecke, K. Wapenaar, and E. Slob, 2015a, Inversion of the multidimensional marchenko equation: Presented at the 77th EAGE Conference and Exhibition 2015.

van der Neut, J., I. Vasconcelos, and K. Wapenaar, 2015b, On green's function retrieval by iterative substitution of the coupled marchenko equations: Geophysical Journal International, **203**, 792–813.

Wapenaar, K., J. Thorbecke, J. Van Der Neut, F. Broggini, E. Slob, and R. Snieder, 2014, Marchenko imaging: Geophysics, **79**, WA39–WA57.